Available online at www.sciencedirect.com
ScienceDirect
Virology 370 (2008) 295–309
VIROLOGY
www.elsevier.com/locate/yviro

Hepatitis C virus NS3/4A protein interacts with ATM, impairs DNA repair and enhances sensitivity to ionizing radiation

Chao-Kuen Lai [a], King-Song Jeng [a], Keigo Machida [b], Yi-Sheng Cheng [a], Michael M.C. Lai [a,b,*]

[a] *Institute of Molecular Biology, Academia Sinica, Taipei, 115, Taiwan*
[b] *Department of Molecular Microbiology and Immunology, University of Southern California, Keck School of Medicine, 2001 Zonal Avenue, Los Angeles, CA 90033, USA*

Received 11 June 2007; returned to author for revision 5 July 2007; accepted 25 August 2007
Available online 10 October 2007

Abstract

Hepatitis C virus (HCV) infection is frequently associated with the development of hepatocellular carcinomas and non-Hodgkin's B-cell lymphomas. Nonstructural protein 3 (NS3) of HCV possesses serine protease, nucleoside triphosphatase, and helicase activities, while NS4A functions as a cofactor for the NS3 serine protease. Here, we show that HCV NS3/4A interacts with the ATM (ataxia-telangiectasia mutated), a cellular protein essential for cellular response to irradiation. The expression of NS3/4A caused cytoplasmic translocation of either endogenous or exogenous ATM and delayed dephosphorylation of the phosphorylated ATM and γ-H2AX following ionizing irradiation. As a result, the irradiation-induced γ-H2AX foci persisted longer in the NS3/4A-expressing cells. Furthermore, these cells showed increased comet tail moment in single-cell electrophoresis assay, indicating increased double-strand DNA breaks. The cells harboring an HCV replicon also exhibited cytoplasmic localization of ATM and increased sensitivity to irradiation. These results demonstrate that NS3/4A impairs the efficiency of DNA repair by interacting with ATM and renders the cells more sensitive to DNA damage. This effect may contribute to HCV oncogenesis.

Keywords: Hepatitis C virus; Nonstructural protein NS3/4A; Double-strand DNA breaks; DNA repair; Ataxia-telangiectasia mutated; γ-H2AX foci; Oncogenesis

Introduction

Hepatitis C virus (HCV) infects more than 170 million people in the world (Shepard et al., 2005). The importance of HCV infection in hepatocellular carcinomas (HCC) and non-Hodgkin's B-cell lymphomas has been well documented (Ferri et al., 1994; Saito et al., 1990). HCV is a unique nonretroviral oncogenic RNA virus and replicates in the cytoplasm of the cells. It does not contain an obvious oncogene and does not integrate into host genomes. The mechanism of its oncogenesis remains largely unclear. HCV contains a 9.6-kb RNA genome that encodes a large polyprotein (>3000 aa), which is cleaved into 10 structural and nonstructural (NS) proteins through the action of cellular proteases as well as the viral-encoded proteases, including NS2 and NS3/4A. NS3 contains serine protease activities that require a cofactor NS4A, which enhances the proteolytic activity of NS3 and is required for *trans*-cleavage at the NS4B/5A junction (Wolk et al., 2000). NS3 also contains a helicase activity.

Previously, we have reported that HCV infection stimulates the production of nitric oxide (NO) through activation of the gene for inducible NO synthase (iNOS) by the viral core and NS3 proteins (Machida et al., 2004). NO causes double-strand DNA breaks (DSBs) and enhances the mutation frequency of cellular genes, including proto-oncogenes and tumor suppressor genes (Machida et al., 2004). More recent studies further showed that HCV infection, through the core, E1, and NS3 proteins, also induced production of reactive oxygen species (ROS), contributing to DSBs (Machida et al., 2006). DSBs are the most harmful form of DNA damage because they lead to chromosomal breakage and rearrangement. DSBs can also be caused by exogenous agents such as ionizing radiation (IR) and by the

* Corresponding author. Institute of Molecular Biology, Academia Sinica, Taipei, 115, Taiwan. Fax: +886 2 27826085.
E-mail address: michlai@gate.sinica.edu.tw (M.M.C. Lai).

0042-6822/$ - see front matter © 2007 Elsevier Inc. All rights reserved.
doi:10.1016/j.virol.2007.08.037

introduction of errors during DNA replication and mitosis. DSBs are recognized by a sensor that transmits signals to a series of downstream effector molecules to activate signaling mechanisms for cell cycle arrest and induction of repair or cell death if the damage is irreparable. The nuclear protein kinase ataxia-telangiectasia mutated (ATM) is regarded as the sensor and transducer of this network (Shiloh, 2003; Shiloh and Kastan, 2001). It is mutated in ataxia-telangiectasia, a genetic disorder

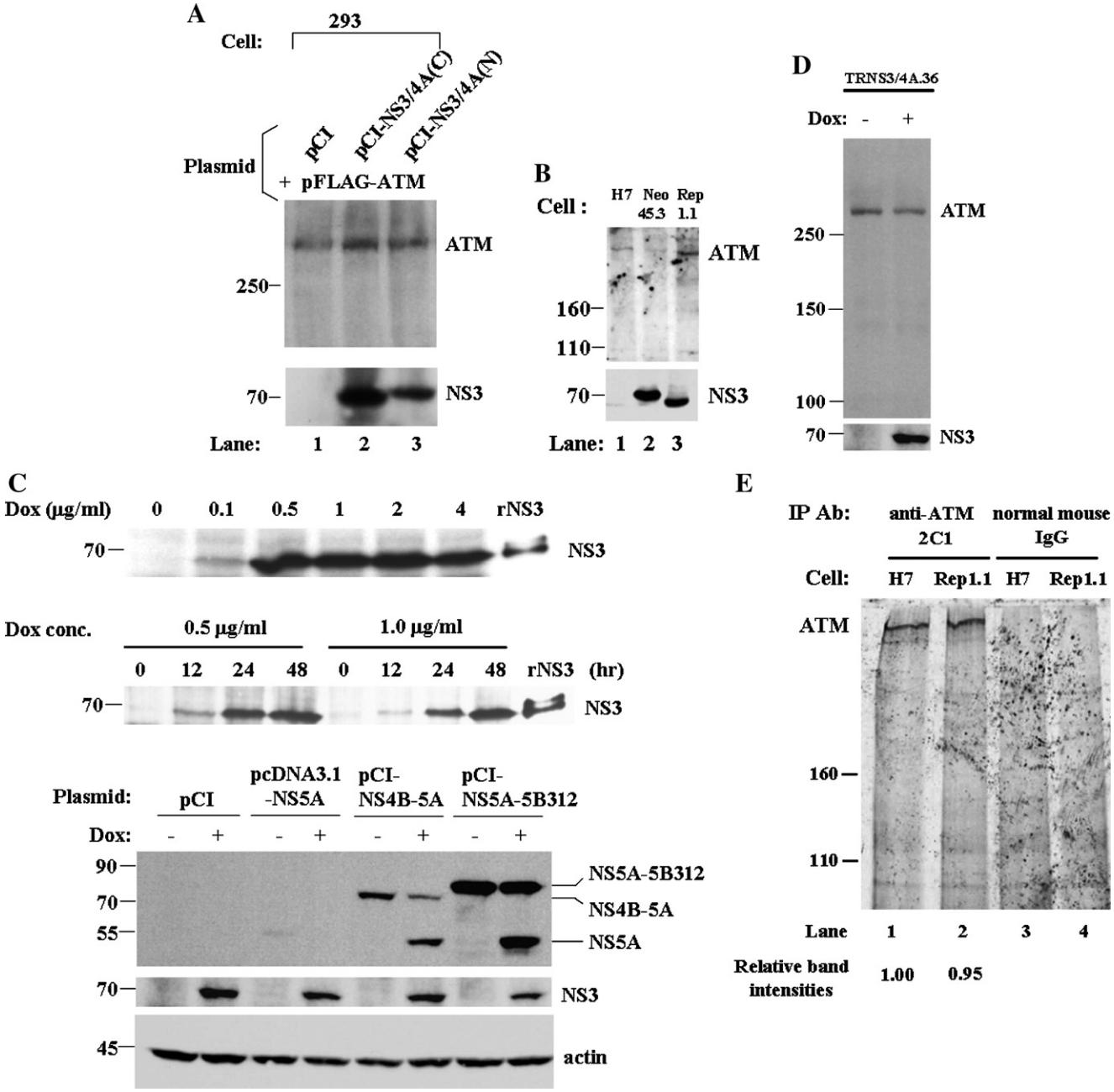

Fig. 1. ATM is not a substrate for NS3/4A protease. (A) HEK293 cells were transfected with FLAG-ATM together with the expression vectors for empty (lane 1), NS3/4A(C) (lane 2), or NS3/4A(N) (lane 3). At 48 h after transfection, cell lysates were resolved by 6% SDS–PAGE and then immunoblotted with MAb (5C2) against ATM or a NS3 MAb. (B) Lysates of naive Huh-7 (lane 1), Neo45.3 (lane 2), and Rep1.1 (lane 3) cells harboring the replicon constructs pUC-HCV1bneo45 (Guo et al., 2001) and pUC-Replicon (Lee et al., 2004), respectively, were immunoblotted with MAbs against ATM and NS3. (C) (Top) TRNS3/4A.36 cells were cultured in the presence of the indicated amounts of Dox (Doxycycline). After 48 h, cell lysates were resolved by SDS–PAGE and then immunoblotted with a MAb against NS3. Recombinant NS3 protein acts as a molecular weight marker. (Middle) NS3/4A expressed at various times after the addition of 0.5 or 1 μg/ml Doxycycline to media. (Bottom) *trans*-Cleavage competence of NS3/4A expressed in the Dox-inducible cell line. TRNS3/4A.36 cells were transfected with an empty vector pCI, or a molecular weight positive control vector pcDNA3.1-NS5A, or NS3 substrate expression vectors pCI-NS4B-5A or pCI-NS5A-5B312, followed by incubation for 48 h in the absence or presence of Doxycycline. NS3 and NS5A were detected by Western blot with an anti-NS3 or -NS5A Ab. (D) TRNS3/4A.36 cell lysates were harvested in the absence or presence of Doxycycline for 48 h and then detected by immunoblot with MAbs against ATM and NS3. (E) Huh-7 and Rep1.1 cells were labeled for 24 h with [^{35}S]-protein labeling mixture; cells were lysed, immunoprecipitated with ATM antibody, and analyzed by autoradiography. Results were quantified by PhosphorImager counting as described in Materials and methods.

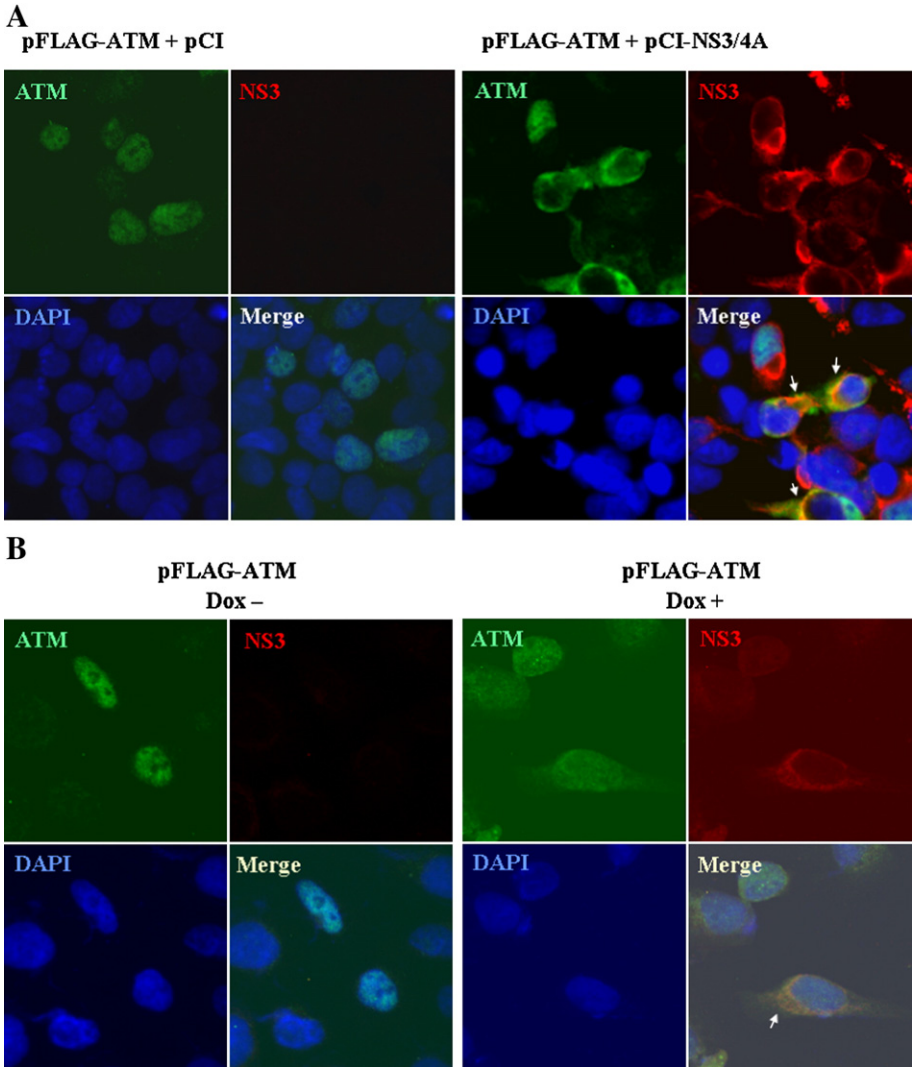

Fig. 2. NS3 partially colocalized with exogenous ATM in the cytoplasm. (A) HEK293 cells were transfected with plasmids pFLAG-ATM and empty vector or pCI-NS3/4A. At 48 h posttransfection, cells were co-stained with rabbit anti-ATM polyclonal Ab (Ab3) (green fluorescence), anti-NS3 mouse MAb (red fluorescence), and DAPI. Confocal images from this experiment were superimposed to demonstrate colocalization (yellow merge fluorescence). Arrows indicate the colocalization of ATM and NS3. (B) One day after seeding, TRNS3/4A.36 cells were transfected with plasmid pFLAG-ATM followed by treatment with or without Doxycycline for 48 h before co-staining with same antibodies and DAPI as in panel A.

characterized by cerebellar degeneration, immunodeficiency, radiation sensitivity, genetic instability, and cancer predisposition (Barzilai et al., 2002), and is essential for rapid induction of cellular responses to DSBs. ATM localizes predominantly in the nucleus of most proliferating cells, with a trace amount residing in the cytoplasm (Brown et al., 1997; Chen and Lee, 1996). Nuclear localization signal of ATM is mapped near the amino terminus (^{385}KRKK^{388}) and is required for the functional activities of ATM (Young et al., 2005). In resting human cells, ATM is present as dimers; exposure to IR induces its autophosphorylation at serine 1981, dimer dissociation, and activation of kinase (Bakkenist and Kastan, 2003). Thereafter, ATM accumulates at sites of DSBs and rapidly phosphorylates histone H2AX at serine 139 (Burma et al., 2001). In mammals, phosphorylation of H2AX plays a critical role in the recruitment of damage-signaling factors to the sites of DNA damage. The phosphorylated H2AX, called γ-H2AX, forms clusters at each DSB site and produces foci that can be observed by immunofluorescence within minutes of IR (Celeste et al., 2003; Rogakou et al., 1999). γ-H2AX is dephosphorylated and removed from chromatin by phosphatase 2A (PP2A). In cells lacking active PP2A, γ-H2AX foci persist much longer than in control cells, and the PP2A-deficient cells have inefficient DNA repair and are hypersensitive to DNA damage (Chowdhury et al., 2005). The rate of disappearance of γ-H2AX foci is reversely correlated with cellular radiosensitivity (Taneja et al., 2004) and reflects the ability of the cells to repair DNA (Chowdhury et al., 2005). Failure of DNA repair leads to genetic instability, which, in turn, may enhance the rate of cancer development (Motoyama and Naka, 2004).

Recent studies have shown that NS3/4A could suppress the host antiviral immune system by cleaving two cellular targets, Toll-IL-1 receptor domain-containing adaptor inducing IFN-β (TRIF) (Li et al., 2005a) and mitochondrial antiviral signaling

(MAVS; also know as IPS-1, VISA, and CARDIF) (Li et al., 2005b; Meylan et al., 2005), involved in the induction of type-I interferons (IFNs), IFN-α, and IFN-β. In order to identify additional potential cellular targets cleavable by NS3/4A, we used the consensus sequence [DE]-x(2)-V-x-[CT]-[SA]-x(2)-[YL] of the *trans*-cleavage site of NS3/4A (see Materials and

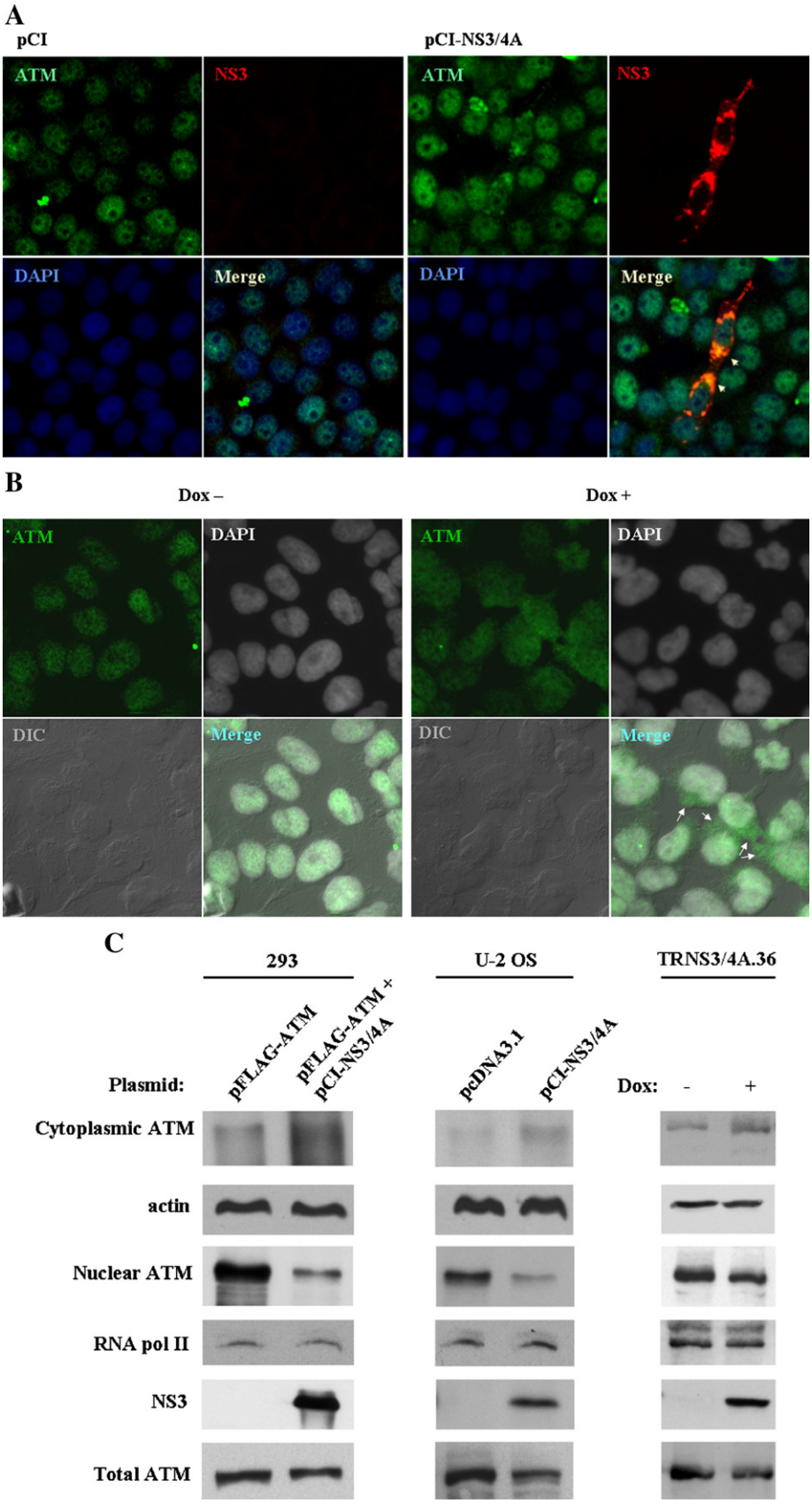

methods) to search for its possible substrates in protein databases. We found that ATM is a potential substrate of NS3/4A. However, we found that NS3/4A could cleave neither endogenous nor exogenous ATM. Nevertheless, NS3/4A co-localized and interacted with ATM. In addition, NS3/4A caused partial translocation of ATM from the nucleus to the cytoplasm and specifically interacted with ATM. Furthermore, following exposure to IR, cells expressing NS3/4A showed delayed dephosphorylation of γ-H2AX and persistence of γ-H2AX foci. In addition, these cells showed increased "comet" tail in single-cell electrophoresis assay, indicating increased double-strand DNA breaks. All of these observed effects were also demonstrated in hepatocytes harboring an HCV replicon. These results demonstrate that NS3/4A can inhibit DNA repair, thus causing DNA damage and contributing to HCV oncogenesis.

Results

ATM contains potential sequences but is not the proteolytic target of NS3/4A

To identify the potential cellular targets of HCV NS3/4A protease, we first analyzed the reported cleavage sites of NS3/4A, NS4A/4B, NS4B/5A, and NS5A/NS5B of HCV and applied ClustalW (Thompson et al., 1994) and ScanProsite (Gattiker et al., 2002) to search for the presence of potential proteolytic targets of NS3/4A among the cellular proteins. Candidate selection was based on the results from bioinformatic analysis. ATM was one of the cellular proteins identified; the potential cleavage site was predicted at amino acid (aa) residues 713 to 722 (sequence ETLVRCSRLL; the conserved residues of *trans*-cleavage sites are underlined). To determine whether ATM is a proteolytic target of NS3/4A, we co-transfected the expression plasmids encoding FLAG-ATM and NS3/4A into HEK293. We then performed immunoblotting for the detection of cleavage products. No cleavage products of ATM were identified in these experiments (Fig. 1A). The similar result was obtained in the cells harboring an HCV subgenomic replicon (Fig. 1B). In addition, we established a tetracycline-regulated cell line, TRNS3/4A.36, expressing NS3/4A complex in the presence of Doxycycline. Fig. 1C shows that NS3 protein expression was induced upon Doxycycline addition and reached a steady-state level at 0.5 to 1 μg/ml or higher concentration of Doxycycline (Fig. 1C, top). NS3 protein expression reached the maximal level after 48 h of treatment (Fig. 1C, middle). Furthermore, when NS4B/5A or NS5A/5B312 was transfected into TRNS3/4A.36 cells, in the presence of Doxycycline, NS5A was released from the precursor (Fig. 1C, bottom), indicating that NS3 is capable of *trans*-cleavage. We therefore used this TRNS3/4A.36 inducible cell line to test whether endogenous ATM could be cleaved by NS3/4A. No cleavage products were identified (Fig. 1D). Even when different anti-ATM antibodies, Ab3 and 2C1, which recognize aa 819–844 and aa 2577–3056 of ATM, respectively, were used, no cleavage products of ATM were identified (data not shown). Next, we further performed metabolic labeling of proteins and then immunoprecipitation by using anti-ATM Ab (2C1) in both Huh-7 naive cells and HCV replicon cells. We found that the amounts of ATM protein were similar, and no cleavage products of ATM were identified in both Huh-7 and HCV replicon cells (Fig. 1E, lanes 1 and 2). We also included a control IP using normal mouse IgG, which did not precipitate ^{35}S-ATM (Fig. 1E, lanes 3 and 4). Taken together, ATM is not a proteolytic target of NS3/4A even though it contains the NS3 consensus cleavage sequences.

HCV NS3/4A induced ATM cytoplasmic localization and partially colocalized with ATM in the cytoplasm

Although we found that ATM was not cleaved by NS3/4A, the presence of the predicted cleavage consensus of NS3/4A in the ATM sequence raised a possibility that ATM may interact with NS3/4A. Therefore, we studied the potential of NS3/4A to alter ATM subcellular localization. pFLAG-ATM was cotransfected together with plasmid pCINS3/4A or an empty vector into HEK293 or TRNS3/4A.36 cells in the absence or presence of Doxycycline. We found that most of the FLAG-ATM proteins were localized within the nucleus in the absence of NS3/4A in either HEK293 or TRNS3/4A.36 cells (Figs. 2A, left, B, left), consistent with the previous reports (Brown et al., 1997; Chen and Lee, 1996). In contrast, in the presence of NS3/4A, FLAG-ATM was localized predominantly in the cytoplasm and partially colocalized with NS3 (Figs. 2A, right, B, right). These results strongly suggest that NS3/4A may induce ATM cytoplasmic translocation. In order to reduce error, self-deception, and bias in the observation of ATM localization, we performed a double-blind test in transfected HEK293 cells. The location of FLAG-ATM was determined in 100 HEK293 cells. The results showed that, in the presence and absence of NS3/4A, the percentage of cells with cytoplasmic ATM was 54% and 6%, respectively. These results provide strong evidence that NS3/4A protein induces translocation of ectopically expressed FLAG-ATM to the cytoplasm.

Next we investigated whether the NS3/4A was also able to induce translocation of endogenous ATM into the cytoplasm. It has been reported that ATM was most abundant in HeLa and U-2 OS cell lines (Gately et al., 1998). Therefore, we transfected pCI-NS3/4A or an empty vector into HeLa cells. We found that most of the endogenous ATM protein was localized within the nucleus in the absence of NS3/4A (Fig. 3A, left), whereas in the presence of NS3/4A, the endogenous ATM was localized also in the cytoplasm, where it was partially colocalized with NS3/4A (shown by yellow in Fig. 3A, right). In TRNS3/4A.36 cells,

Fig. 3. NS3 partially colocalized with endogenous ATM in the cytoplasm. (A) HeLa cells were transfected with an empty plasmid or plasmid pCI-NS3/4A. At 48 h posttransfection, cells were co-stained with anti-ATM rabbit polyclonal Ab (Ab3), anti-NS3 mouse MAb, and DAPI. (B) One day after seeding, TRNS3/4A.36 cells were treated with 1 μg/ml of Doxycycline or untreated for 48 h before co-staining with anti-ATM MAb (5C2) and DAPI. (C) ATM- and NS3/4A-transfected HEK293, NS3/4A-transfected U-2 OS, and Doxycycline-treated TRNS3/4A.36 cells were fractionated to yield nuclear and cytoplasmic fractions. ATM and NS3 were detected by immunoblot analysis. Blots were also probed with an Ab against the large subunit of RNA polymerase II or an anti-actin Ab, respectively, as loading and fractionation controls.

whose parental cell is U-2 OS, most of the endogenous ATM was nuclear in the absence of Doxycycline (Fig. 3B, left), whereas, in the presence of Doxycycline, endogenous ATM was also detected in the cytoplasm (Fig. 3B, right). This observation was reproducible in repeated experiments (data not shown). Taken together, these results show that the HCV NS3/4A can promote ATM translocation into the cytoplasm and is partially colocalized with ATM.

To further confirm that NS3/4A induces cytoplasmic translocation of ATM, we performed biochemical fractionation of cell lysates into cytoplasmic and nuclear fractions and determined the relative distribution of ATM in these fractions. As shown in Fig. 3C, in the absence of NS3/4A, ATM was found predominantly in the nuclei, with small amounts residing in the cytoplasm. In the presence of NS3/4A, ATM was relatively more abundant in the cytoplasmic than the nuclear fractions. These data indicate that ATM is partially translocated into the cytoplasm in the presence of NS3/4A.

HCV NS3/4A physically interacts with ATM

Since immunostaining of NS3 and ATM showed their colocalization in the cytoplasm, we investigated whether HCV NS3 could form a complex with ATM. Total lysates from either NS3/4A-transfected HeLa or NS3/4A-ATM-cotransfected HEK293T were precipitated with anti-HA beads and then analyzed by immunoblotting using Abs against either ATM or NS3. The results showed that ATM specifically coprecipitated with HCV NS3 protein (Figs. 4A, B). When the cytoplasmic extracts from Doxycycline-treated TRNS3/4A.36 cells were precipitated with anti-ATM (2C1), a small amount of the endogenous ATM was also coprecipitated with NS3 (Fig. 4C). Control immunoprecipitations using transfected HeLa cells expressing the non-tagged NS3/4A did not precipitate ATM when anti-HA was used for immune precipitation (Fig. 4A, lane 5), indicating the specificity of the observed HCV NS3–ATM interaction. Taken together, these findings indicate that HCV NS3 protein forms a complex with ATM.

HCV NS3/4A delays the dephosphorylation of phospho-Ser1981-ATM and phospho-Ser139-H2AX (γ-H2AX) and the rate of loss of γ-H2AX foci after ionizing radiation

ATM activation involves its autophosphorylation on Ser1981, and this autophosphorylated species produces ionizing-radiation-induced foci that colocalize with the phosphorylated form of histone H2AX, γ-H2AX (Bakkenist and Kastan, 2003; Burma et al., 2001). In addition, nuclear ATM is required for its functional activities, including kinase activity and DNA repair (Young et al., 2005). The data shown above indicate that HCV NS3/4A promotes ATM translocation into the cytoplasm

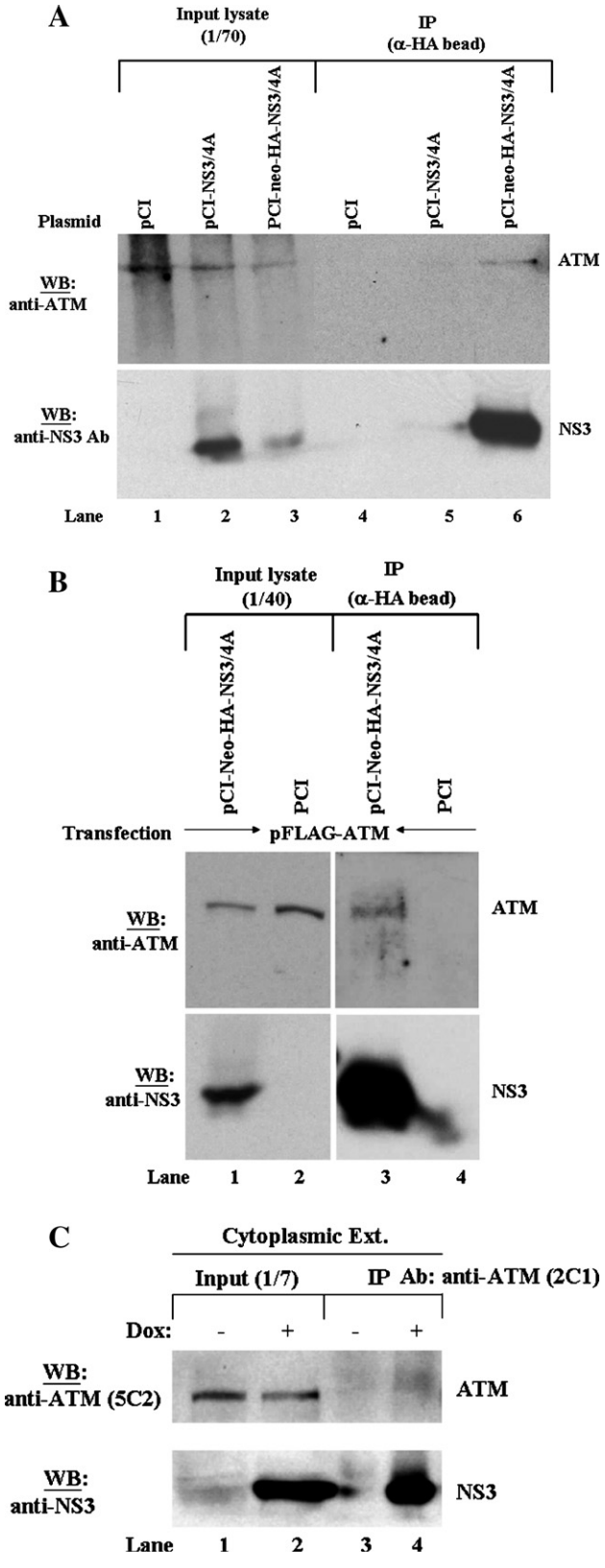

Fig. 4. HCV NS3 interacts with ATM. (A) HeLa cells were transfected with NS3/4A, HA-NS3/4A, or empty vector and then immunoprecipitated with the anti-HA bead. The immunoprecipitates and 1/70 of the total cell lysates were blotted against anti-ATM and anti-NS3 MAbs. (B) HEK293T cells were transfected with FLAG-ATM together with HA-NS3/4A or empty vector and then immunoprecipitated with anti-HA bead. The immunoprecipitates and 1/40 of the total cell lysates used were blotted against anti-ATM and anti-NS3 MAbs. (C) TRNS3/4A.36 cells were either untreated or treated for 48 h with Doxycycline. Cytoplasmic lysates were subjected to immunoprecipitation (IP) using ATM antibody (2C1). Immunoprecipitates were blotted with anti-ATM (5C2) and anti-NS3 MAbs, using 1/7 of the input cell lysates.

and colocalizes and interacts with ATM. Therefore, we investigated whether the functional activities of ATM is affected by NS3/4A. The extents of phosphorylation of ATM and histone H2AX were analyzed in TRNS3/4A cells at various time points following ionizing radiation (IR). The extents of their phosphorylation were similar in the presence or absence of NS3 during the first 30 min following IR. However, dephosphorylation of pS1981-ATM and γ-H2AX at 2 h, 4 h, and 24 h post-IR was delayed in the presence of NS3/4A (Fig. 5A). Because protein phosphatase 2A (PP2A) is involved in the dephosphorylation of ATM (Goodarzi et al., 2004) and γ-H2AX (Chowdhury et al., 2005), we further examined the protein levels of PP2A(C) after IR. Surprisingly, the protein level of PP2A was not markedly affected by NS3/4A within 24 h post IR in either unirradiated or irradiated cells (Fig. 5A).

Next we determined whether the formation of γ-H2AX foci was also affected by NS3/4A. The inducible TRNS3/4A.36 cells were irradiated with 2 or 5 Gy IR in the absence or presence of Doxycycline and then processed for image analysis. In the absence of IR, very few γ-H2AX foci (<5 foci/cell) were present in the nuclei in either Doxycycline-untreated or -treated cells (Figs. 5B, C). This finding was consistent with the previous report (Buscemi et al., 2004) that the basal number of foci per cells is 2.8±0.9. The number of foci per cell increased to over 40 at 15 min after 2 or 5 Gy IR. Thereafter, the number decreased in Doxycycline-untreated cells; by 24 h post IR, the number of foci was similar to that in the unirradiated cells (Figs. 5B, C). By comparison, in Doxycycline-treated cells, the number of foci per cells showed a significantly slower rate of decline (Figs. 5B, C). These results are consistent with the results seen with immunoblot analysis (Fig. 5A). As a control, Doxycycline treatment alone without irradiation did not induce γ-H2AX foci in the nucleus (data not shown).

DNA damage-induced γ-H2AX foci represent sites of DNA DSBs and can be used to detect DSBs semiquantitatively by immunofluorescence microscopy (Rothkamm and Lobrich, 2003). Therefore, the total numbers of foci present in 200 cells were counted in each experiment. Significantly, in the presence of NS3/4A, the percentages of cells with >5 foci/cell after 24 h and 48 h with 2 Gy IR were 18% and 17%, respectively, whereas in the absence of NS3/4A, they were 5% and 4%, respectively (data not shown). The numbers at 5 Gy were 41% and 37% in the presence of NS3/4A vs. 14% and 13% in the absence of NS3/4A (data not shown). Since the rate of loss of the foci correlates with the rate of DSBs repair, this finding supports the idea that DSBs are not efficiently repaired if cells express HCV NS3/4A protein.

NS3/4A-expressing cells are defective in DNA repair and are hypersensitive to ionizing radiation

To corroborate the immunofluorescence data, we used the neutral comet assay to determine whether NS3/4A expression affected DNA repair. TRNS3/4A cells were treated with Doxycycline and irradiated (10 Gy). After 1 h with IR, comet tail formation was observed clearly, and the tail appearance was similar in both Doxycycline-treated and -untreated cells. However, the tail was no longer observed in the control population by 24 h, whereas tails were still visible in NS3/4A-expressing cells (Fig. 6A). The comet tail moments of Doxycycline-treated cells were also significantly more abundant than that of untreated cells, particularly after 24 h following IR (Fig. 6B). Based on the comet moments, which quantify the extent of DNA damage, we estimate 4- to 5-fold more unrepaired DNA damage in NS3/4A-expressing cells than control cells at 24 h (Fig. 6B). These results are comparable with those seen in γ-H2AX foci formation (Figs. 5B, C). Taken together, this finding provides further evidence that HCV NS3/4A impairs the efficiency of DNA repair and induces hypersensitivity to DNA damage.

HCV replicon cells have cytoplasmic ATM and are defective in DNA damage repair

To demonstrate that the findings reported above are relevant to HCV replication, we repeated most of the experiments in a Huh-7 cell line, Rep 1.1, harboring an HCV subgenomic replicon (Lee et al., 2004). The subgenomic RNA encodes most of HCV NS proteins, including NS3/4A protease. However, the amount of ATM was too low in Huh-7 cells to be detected by immunofluorescence staining. Therefore, exogenous pFLAG-ATM was introduced into the replicon cells. While FLAG-ATM was localized in the nucleus of Huh-7 cells (Fig. 7), it was detected in both the nucleus and the cytoplasm, where it was partially colocalized with NS3/4A, in HCV replicon cells (shown by yellow in Fig. 7, right). This observation was reproducible in repeated experiments (data not shown).

We next examined the radiosensitivity of the HCV replicon cells. Huh-7 and Rep 1.1 cells were irradiated with 5 Gy IR. In the absence of IR, very few γ-H2AX foci (<5 foci/cell) were present in either Huh-7 or Rep 1.1 cells. The number of foci per cell increased to over 40 at 15 min after IR. Thereafter, the number decreased in Huh-7 cells; at 24 h post IR, the number of foci was similar to that in the unirradiated cells (Figs. 8A, B). By comparison, in HCV replicon cells, the number of foci per cells showed a significantly slower rate of decline (Fig. 8). As a control, the G418 treatment alone without irradiation did not induce γ-H2AX foci (data not shown). We also determined the percentages of cells with increased γ-H2AX foci after irradiation. In HCV replicon cells, the percentages of cells with >5 and >10 foci/cell after 4 h with 5 Gy IR were 97% and 84%, respectively, whereas in Huh-7 cells, they were 78% and 60% (Fig. 8C). The numbers at 24 h were 33% and 24% in HCV replicon cells vs. 17% and 3%, respectively, in Huh-7 cells (Fig. 8C, bottom). These results are similar to the results of irradiated TRNS3/4A.36 cells (Figs. 5B, C). We conclude that NS3-induced defects in DNA damage repair are relevant to HCV replication.

Discussion

Bioinformatic analysis suggested that ATM is a potential target of the proteolytic activity of HCV NS3 protein. However, although ATM contains a conserved cleavage site of NS3/4A protease at P1 (^{718}Cys), P1′ (^{719}Ser), and P6 (^{713}Glu) residues,

ATM was not cleaved in cells expressing NS3/4A. Previous studies have shown that the cleavage targets of NS3/4A, TRIF, and MAVS lack a perfect cleavage site and yet are cleaved (Li et al., 2005a,b; Meylan et al., 2005). In contrast, RIG-I has a consensus NS3 cleavage sequence and yet is not cleaved (Foy et al., 2005; Meylan et al., 2005). Nevertheless, our results

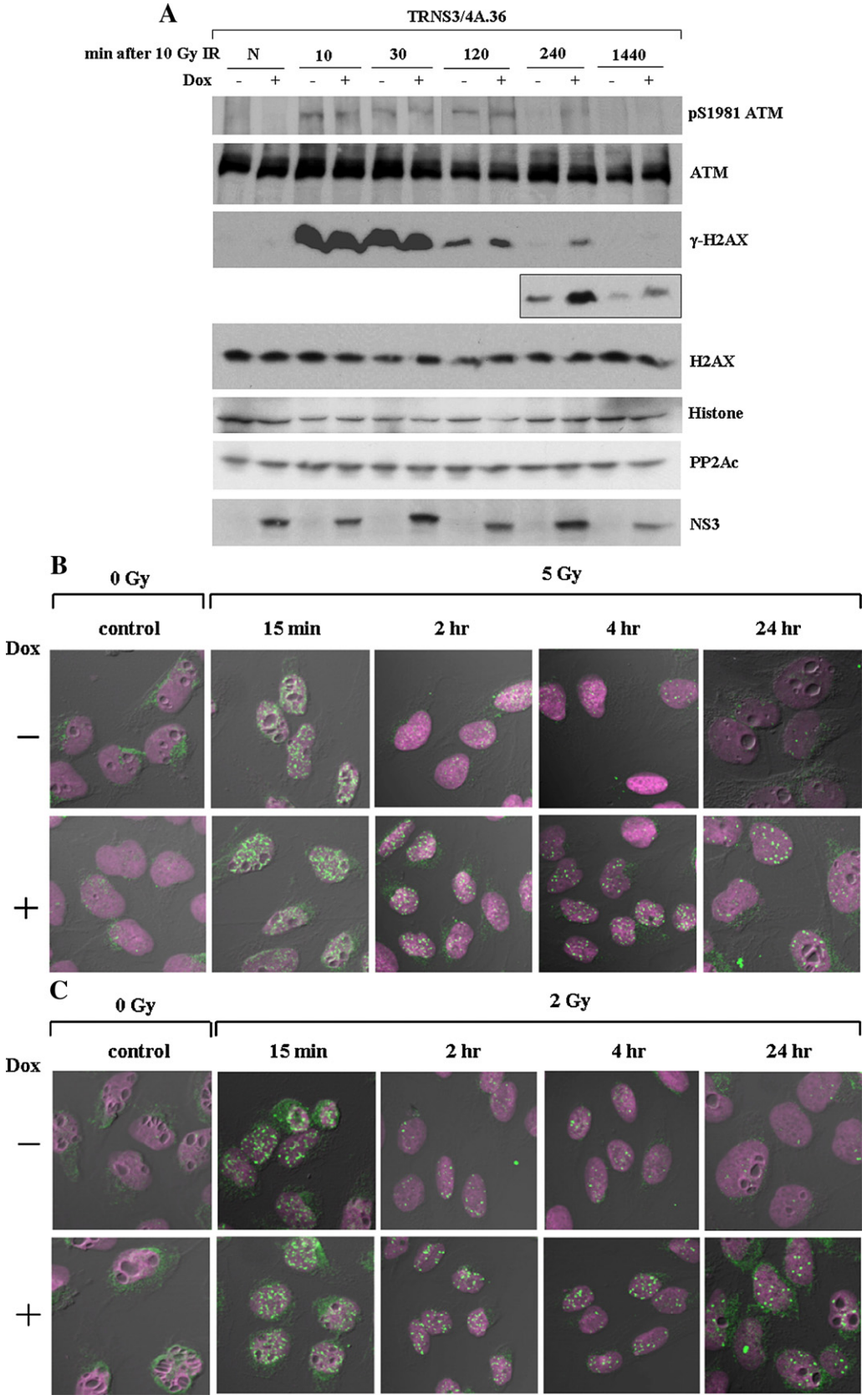

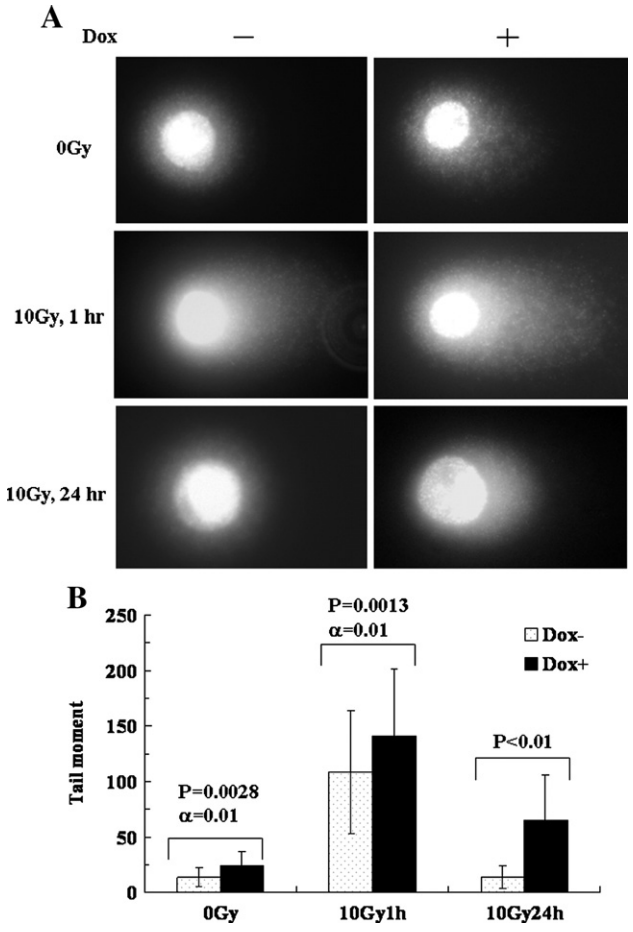

Fig. 6. HCV NS3/4A impairs the efficiency of DNA damage repair. (A) TRNS3/4A cells were treated or untreated with Doxycycline. After 48 h, cells were analyzed by neutral comet assay at the indicated time points following IR (10 Gy). (B) The comet tail moment of 50 cells (mean±SD) of Doxycycline-treated NS3/4A-expressing cells relative to those in untreated cells is shown after exposure to IR. Color coding is as follows: white bars, untreated cells; black bars, Doxycycline-treated cells.

showed that, similar to RIG-I, the ATM pathway is targeted by NS3/4A, thereby allowing HCV to impair the DNA repair in cells.

In proliferating cells, ATM localizes predominantly in the nucleus, with a small amount being present in the cytoplasm. By contrast, in human and mouse Purkinje cells, ATM is localized mainly in the cytoplasm, and its absence leads to abnormalities of cytoplasmic organelles (Barlow et al., 2000; Oka and Takashima, 1998). In proliferating cells, the biological function of ATM in the cytoplasm is still unknown (Brown et al., 1997; Chen and Lee, 1996; Lim et al., 1998; Watters et al., 1999), but its nuclear localization is required for its functional activities, including kinase activity and DNA repair (Young et al., 2005). When NS3 was expressed alone, it was diffusely distributed in both the cytoplasm and the nucleus; in contrast, when NS3 was co-expressed with NS4A, the majority of the NS3 protein was localized in the cytoplasm (Muramatsu et al., 1997; Wolk et al., 2000). The present study demonstrated that the cytoplasmic NS3 partially colocalized with ATM. Biochemical studies also showed that there was a physical interaction between NS3 and ATM. Furthermore, these interactions were demonstrated in hepatocytes harboring an HCV replicon. How the cytoplasmic NS3/4A can interact with the nuclear ATM is an interesting question. There are two possible mechanisms: first, NS3 interacts either directly or indirectly with newly synthesized ATM in the cytoplasm and inhibits the nuclear translocation of ATM by blocking the nuclear localization signal. Second, some NS3 may be localized in the nuclei even in the presence of NS4A (Deng et al., 2006; Muramatsu et al., 1997) and interact with nuclear ATM: the NS3–ATM complexes are then transported to the cytoplasm by an unknown mechanism. The latter interpretation may explain why only a minor fraction of ATM in the cytoplasm interacted with NS3 (Figs. 3C and 4). We have further observed that the protease activity is not required for the NS3–ATM interaction (data not shown).

As a result of ATM retention in the cytoplasm, the amount of ATM protein in the nuclei of cells expressing NS3/4A was substantially lower than that in the normal cells (Fig. 3C). Nevertheless, the NS3/4A-expressing cells still exhibit a normal response to DNA damage after exposure to IR (Fig. 5). These results are in agreement with the previous finding (Young et al., 2005) that only a small amount of nuclear ATM is sufficient to mount a normal response to DNA damage. Therefore, the amount of phosphorylated ATM is not a rate-limiting factor in the cellular DNA damage response (Gately et al., 1998). In contrast, NS3/4A-expressing cells and HCV replicon cells showed delayed dephosphorylation of γ-H2AX and the persistence of γ-H2AX foci and, correspondingly, impaired DNA repair activity (Figs. 5 and 8). We suggest that NS3/4A induces deficiency of DSB repair by interfering with the signaling cascade of ATM and H2AX dephosphorylation. However, the amount of PP2A, which has been reported to dephosphorylate ATM and γ-H2AX (Chowdhury et al., 2005; Goodarzi et al., 2004), was not altered in the NS3/4A-expressing cells (Fig. 5A). Further studies defining the effect of NS3/4A on other DSB repair proteins at γ-H2AX foci may help to delineate the mechanism of suppression of DNA repair by NS3/4A.

As shown in Figs. 6A and B, even in unirradiated-NS3/4A-expressing cells, the comet tail moment in the single-cell electrophoresis assay was slightly longer than that in control cells without NS3/4A. These data indicate that NS3/4A may induce some DSBs in unirradiated cells, consistent with our previous reports (Machida et al., 2004, 2006) that NS3/4A

Fig. 5. NS3/4A delayed the dephosphorylation of pS1981-ATM and γ-H2AX and showed persistence of γ-H2AX foci in response to irradiation. (A) The inducible TRNS3/4A cells were untreated (control) or treated with Doxycycline. At 48 h later, cells were analyzed at the indicated time points following IR (10 Gy) using antibodies against phosphorylated ATM (Ser1981) (upper panel) or phosphorylated H2AX (Ser139) (γ-H2AX) (third panel). Also shown are total ATM (second panel), total H2AX (fourth panel), PP2A(C) (sixth panel), NS3 (lower panel), and histone, used as a loading control (fifth panel). Membrane was exposed to film for a longer time (inset). (B) (C) γ-H2AX foci in irradiated cells. Untreated or Doxycycline-treated TRNS3/4A.36 cells were analyzed at the indicated time points following 5 Gy IR (B) or 2 Gy IR (C). Cells were stained with anti-γ-H2AX and DAPI.

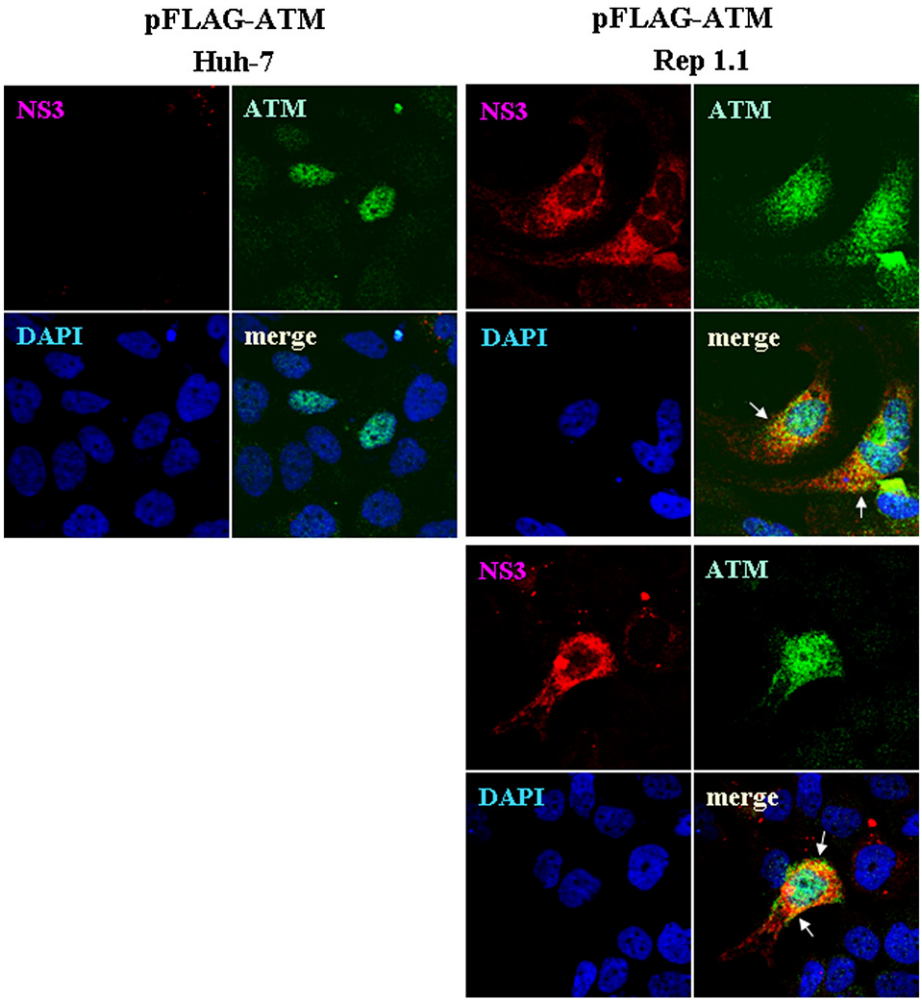

Fig. 7. NS3 partially colocalized with exogenous ATM and induced its cytoplasmic translocation in an HCV replicon cell line (Rep 1.1). Huh-7 and Rep 1.1 cells were transfected with plasmid pFLAG-ATM. At 48 h posttransfection, cells were co-stained with anti-ATM rabbit polyclonal Ab (Ab3) (green fluorescence), anti-NS3 mouse MAb (red fluorescence), and DAPI. Arrows indicate the colocalization of ATM and NS3.

stimulates the production of NO (Machida et al., 2004) and ROS (Machida et al., 2006) and thereby causes DSBs. However, we did not observe significant increase of γ-H2AX foci formation (>5 foci/cell) in unirradiated-NS3/4A-expressing cells (Figs. 5B, C). One possible interpretation is that the extent of DSB induced by NS3/4A is not sufficient to induce full activation of ATM. Very likely, the comet tail moment assay and ligation-mediated PCR for detecting DSBs are more sensitive than the quantification of γ-H2AX foci.

The effects of NS3/4A on DNA repair activity were demonstrated not only in the cells expressing NS3/4A alone, but also in the hepatocytes expressing an HCV replicon. Recently, we further used an infectious HCV (SB virus strain) (Sung et al., 2003) to infect a B-cell lymphocyte cell line and showed that the cells experimentally infected with HCV also showed impaired DNA damage repair activities (data not shown). These results showed that the impairment of DNA damage repair by NS3 is relevant to HCV pathogenesis. This effect will make HCV-infected cells more prone to mutations. In addition, NS3 induces DSBs and activation of STAT3 (Machida et al., 2006), the combination of which may contribute to cell transformation and oncogenesis (Bowman et al., 2000; Frank, 1999). Therefore, the combined effects of NS3/4A and other viral factors (such as core and E1 protein) may synergistically increase the probability of malignant transformation of HCV-infected cells.

Materials and methods

Search for candidates for NS3/4A cleavage by bioinformatic analysis

The non-redundant data set and the sequences of the various HCV polyprotein precursors were extracted from HCV database

Fig. 8. HCV replicon cells showed persistence of γ-H2AX foci in response to irradiation and impaired DNA damage repair activity. Huh-7 or Rep 1.1 cells were examined at the indicated time points following IR (5 Gy). Cells were stained with anti-γ-H2AX and DAPI and are shown at 945× (A) and 441× (B) magnification. (C) The percentages of cells with >5 or >10 foci/cell at 15 min, 4 h, and 24 h following 5 Gy IR.

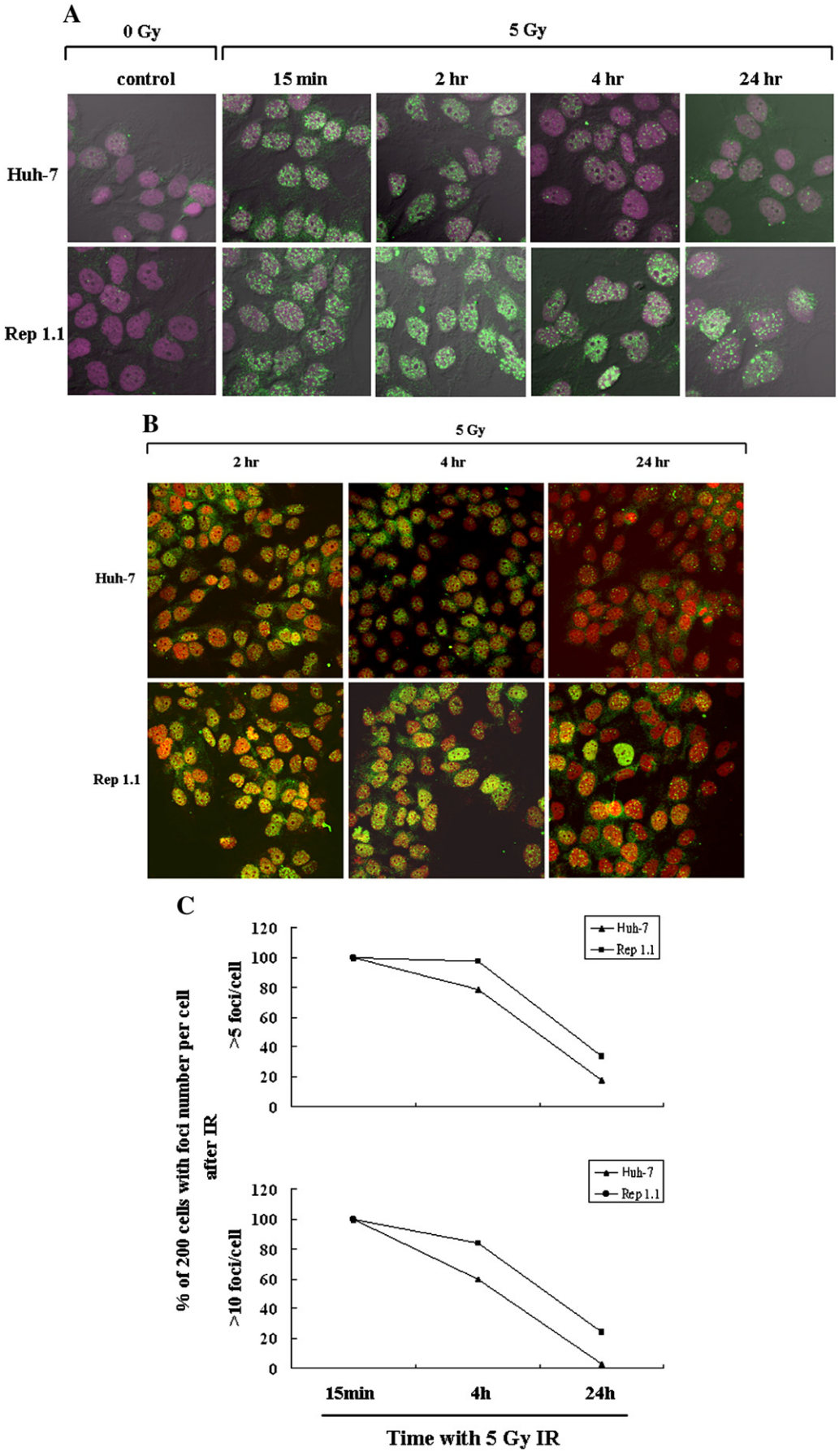
A
0 Gy
5 Gy
control
15 min
2 hr
4 hr
24 hr
Huh-7
Rep 1.1
B
5 Gy
2 hr
4 hr
24 hr
Huh-7
Rep 1.1
C
% of 200 cells with foci number per cell after IR
>5 foci/cell
>10 foci/cell
120
100
80
60
40
20
0
Huh-7
Rep 1.1
15min
4h
24h
Time with 5 Gy IR

(Kuiken et al., 2005). The various cleavage sites (NS3/NS4A, NS4A/NS4B, NS4B/NS5A, and NS5A/NS5B) within the HCV polyprotein targeted by the NS3 serine protease were extracted between P10 and P10′ from filtered sequences. Those sequences were subjected to ClustalW (Thompson et al., 1994) to perform sequence alignment and then to visualize in Weblogo (Crooks et al., 2004). From the results of Weblogo and previous experiment (Narayanan et al., 2002), we generated several different combinations of pattern to search for human proteins that may be cleaved by NS3/4A, in ScanProsite (Gattiker et al., 2002). Protein expression in the human liver was further used as a criterion to filter the scanning results. Finally, a candidate protein ATM was identified by the pattern of Prosite [DE]-x(2)-V-x-[CT]-[SA]-x(2)-[YL].

Cells and media

Huh-7, HeLa, HEK293, and HEK293T were cultured in Dulbecco's Modified Eagle's Medium containing 10% fetal bovine serum (FBS). Two clones of Huh-7/replicon cells, Neo45.3 and Rep 1.1, harboring an HCV subgenomic replicon RNA, were derived from the HCV-N (Guo et al., 2001) and -Con1 strains (Lee et al., 2004), respectively. They were grown in the same medium containing 0.5 mg/ml of G418. Tetracycline (tet)-regulated osteosarcoma U-2 OS cell line TRNS3/4A.36 was generated as previously described (Machida et al., 2006). To induce NS3/4A expression, the cells were treated with 1 μg/ml Doxycycline (BD Biosciences Clontech) and incubated for 48 h.

Plasmids

The plasmids expressing the various HCV proteins were constructed by inserting HCV NS3/4A, NS4B/5A, and 5A/5B312 cDNA of genotype 1b into pCI (Promega) downstream of both the cytomegalovirus (CMV) immediate-early (IE) enhancer/promoter region and a chimeric intron that is composed of the donor site from the first intron of the human β-globin gene and the branch and acceptor site from the intron of an immunoglobulin gene. Plasmids pCI-NS3/4A (N) and pCI-NS3/4A(C) contain the NS3/4A cDNA insert of the HCV-N and -Con1 strains, respectively. Plasmids pCI-NS4B-5A and pCI-NS5A-5B312 express the full-length NS4B-5A and NS5A plus the amino-terminal 312 aa of NS5B, respectively, to serve as substrates for NS3 *trans*-cleavage assays. Plasmid pcDNA3.1-NS5A has been described previously (Tu et al., 1999). To generate the hemagglutinin (HA)-tagged NS3/4A construct (pCI-neo-HA-NS3/4A), the *Xho*I (fill-in of 3′-recessed ends)–*Xba*I fragment containing the NS3/4A cDNA insert of pCI-NS3/4A(C) was cloned into *Eco*RV and *Xba*I sites of the pHA-AT vector such that the N-terminal HA epitope was fused in frame with NS3/4A. The pHA-AT vector was constructed by using annealed oligonucleotides 5′-gctagcctcgagaattcttaattaaaccatg*tacccatacgatgttccagattacgct*ccgatatc*tacccatacgatgttccagattacgct*ctctagagtcgaccgggcggccgc-3′(the *Nhe*I and *Not*I sites are underlined, the engineered translation initiation codon and amber stop codon are double-underlined, the HA-tagged sequence is in italics, and the *Eco*RV site for cloning is bold-underlined), which was cloned into *Nhe*I and *Not*I sites of pCI-neo (Promega). The S139A mutant of NS3/4A was generated by using the jumping PCR method (Higuchi et al., 1988). The protocol was as follows: cDNA fragments comprising nt 3621 to 3850 and nt 3831 to 4414 of the HCV-con1 strain were amplified by PCR from pCI-neo-HA-NS3/4A by using the primer pairs sense 5′-aagggcccaatcacccaaat-3′ and antisense 5′-gcagtggaccgcccgcagagccccttcaagt-3′ (the mutated site is double underlined), as well as sense 5′-acttgaagggctctgcgggcggtccactgc-3′ (the mutated site is double underlined) and antisense 5′-gcacggtgaccgatcccgga-3′. The amplification products were reamplified by using the primer pair sense 5′-aagggcccaatcacccaaat-3′ (the *Apa*I site is underlined) and antisense 5′-gcacggtgaccgatcccgga-3′ (the *Bst*EII site is underlined). Amplification products were cloned into the *Apa*I–*Bst*EII sites of pCI-neo-HA-NS3/4A. To obtain better expression, the resulting plasmids, pCI-neo-HA-NS3/4A and pCI-neo-HA-S139A NS3/4A, were digested with *Xho*I and *Xba*I and then cloned into *Xho*I and *Xba*I sites of the pCI vector to generate pCI-HA-NS3/4A and pCI-HA-S139A NS3/4A, respectively. Plasmid pcDNA3-FLAG-ATM was kindly provided by Dr. Michael B. Kastan (St. Jude Children's Research Hospital) (Lim et al., 1998). All plasmids were verified by DNA sequencing.

Antibodies

The NS3-specific mouse monoclonal antibodies (MAbs) used in immunofluorescence staining were purchased from Vector Laboratories (Burlingame, CA, USA), while mouse anti-NS3 monoclonal antibody used for immunoblotting was from Novocastra Laboratories (Newcastle, UK). The mouse MAb against NS5A was purchased from Biodesign. The mouse MAb against RNA polymerase II was purchased from Covance. The rabbit polyclonal Ab (Ab-3) against ATM used for immunofluorescence staining was from Calbiochem, whereas the mouse ATM-specific MAbs 5C2 and 2C1 used for immunoblotting and immunofluorescence staining and immunoprecipitations, respectively, were from Genetex. Anti-pSer1981-ATM was obtained from Rockland Immunochemicals. Anti-H2AX and anti-PP2A were acquired from Upstate Cell Signaling Solutions. The rabbit polyclonal Ab against γ-H2AX used for immunofluorescence staining was from Trevigen Inc., whereas mouse MAb against γ-H2AX used for immunoblotting was from Upstate Cell Signaling Solutions. Anti-actin and anti-histone antibodies were purchased from Chemicon. Anti-rabbit and anti-mouse secondary antibodies were purchased from Invitrogen Molecular Probes.

Immunoblot

Proteins were resolved by electrophoresis in sodium dodecyl sulfate–polyacrylamide gels (SDS–PAGE) and electrophoretically transferred onto polyvinylidene difluoride membranes (Hybound-P; Amersham Bioscience). The membranes were

incubated with primary antibodies and then reacted with peroxidase-conjugated secondary antibodies. Immunoreactivity was visualized by an enhanced chemiluminescence detection system (Amersham Bioscience) or a SuperSignal West Femto detection system (Pierce).

Immunofluorescence staining

Cells cultured on glass chamber slides (Lab-Tek II) were washed twice with PBS, fixed with 4% paraformaldehyde for 20 min, and then permeabilized in cold acetone for 3 min. Primary antibodies were diluted in 5% bovine serum albumin (BSA) and incubated with cells for 1 h at 37 °C. After three washes in PBS, fluorescein- and/or rhodamine-conjugated secondary antibodies were added to cells for 1 h at 37 °C. Nuclear staining by 4′,6′-diamidino-2-phenylindole dihydrochloride (DAPI) (Sigma-Aldrich) was performed by mixing DAPI (0.5 μg/ml) with the secondary antibody. After staining, slides were washed in PBS and mounted in ProLong Antifade (Invitrogen Molecular Probes). Photographs of the cells were taken with a confocal microscope (Zeiss Confocal Laser Scanning Microscope LSM 510). Image analysis was performed using the standard system operating software provided with the microscope. To allow direct comparisons, all of the images were captured using the same parameters. In double-blind test, the number (%) of cells with either intranuclear or cytoplasmic ATM proteins was counted by using the confocal microscopic images obtained using a ×63 objective lens. The foci of phosphorylated H2AX were similarly determined. A total of 200 cells were counted in each experiment. Foci number at >5 foci/cell was considered as significant.

Subcellular fractionation

Cytoplasmic and nuclear fractions were prepared from asynchronously growing cells using an NE-PER Nuclear-cytoplasmic kit (Pierce) according to the manufacturer's instructions. The purity of each fraction was analyzed by immunoblotting using antibodies against RNA polymerase II and actin. Cytoplasmic and nuclear fractions containing 60 μg and 20 μg of protein, respectively, were resolved by SDS–PAGE and transferred to polyvinylidene difluoride membranes (Hybond-P; Amersham Bioscience) for immunoblotting.

Coimmunoprecipitations

TRNS3/4A.36 cell line was grown in the presence or absence of Doxycycline. Cytoplasmic extracts were prepared for each sample according to the NE-PER protocol (Pierce). Ten micrograms of ant-ATM antibody (2C1, Genetex) was incubated with cytoplasmic lysates overnight at 4 °C. Five microliters of Protein-A magnetic beads (NEB) was then added and the mixture incubated for an additional 1 h at 4 °C to capture the ATM–antibody complex. For detection of the interactions between the endogenous or exogenous ATM proteins with anti-HA-NS3/4A beads, total lysates were prepared according to Profound Mammalian HA-Tag IP/Co-IP kit (Pierce). The immunoprecipitated proteins were run on a 6% SDS–polyacrylamide gel, and immunoblot analysis was performed for ATM protein and NS3 protein by using secondary anti-ATM (5C2, Genetex) and -NS3 (Novocastra) antibodies, respectively.

Metabolic labeling and immunoprecipitation

Cell monolayers were metabolically labeled by starving them in methionine- and cysteine-free medium (Life Technologies, Rockville, MD) for 1 h and thereafter labeling with 50 μCi/ml of both [^{35}S]methionine and [^{35}S]cysteine (Perkin-Elmer, NEN Life Science Products, Boston, MA) for 24 h. Cells were harvested and washed twice with PBS. Immunoprecipitation was performed as described above. The immunoprecipitated proteins were separated by electrophoresis on a 6% SDS–polyacrylamide gel and quantified using a Fuji PhosphorImager (FLA-5000; Fuji Photo Film Co., Tokyo, Japan).

Neutral single-cell electrophoresis (comet) assay

Neutral comet assay was performed using the CometAssay kit (Trevigen Inc.). Briefly, TRNS3/4A.36 cells were cultured in the presence or absence of Doxycyline for 48 h and then exposed to γ-ray (10 Gy). The treated cells were resuspended in ice cold PBS at 1×10^5/ml. A 50-μl aliquot of this suspension was mixed with 0.5 ml of prewarmed 1% low-melting-point agarose, and 75 μl was pipetted immediately onto a CometSlide. The slides were placed in refrigerator for 10 min and then immersed in prechilled lysis solution at 4 °C for 30 min. After washing with Tris–borate EDTA buffer, slides were then subjected to electrophoresis for 20 min at 1 V/cm. After electrophoresis, slides were air-dried and stained with SYBR Green dye. Nuclei were visualized under a fluorescence microscope (Carl Zeiss Axiovert 200). The images of nuclei were captured using a charge-coupled device camera (CoolSANP-HQ) and analyzed with the Kinetic Imaging Software Komet 5.5. For each sample, 50 randomly chosen cells were scored for tail moment. Relative tail moments in Doxycycline-treated cells were compared with these in untreated cells.

Statistical analysis

Statistical comparisons between groups were made using a two-sample Kolmogorov–Smirnov (KS) test. The difference was considered to be statistically significant when p was <0.05.

Acknowledgments

We thank Dr. Michael B. Kastan of St. Jude Children's Research Hospital, USA, for FLAG-ATM expression vector, Dr. Ching-Huang Lai from National Defense Medical Center, Taiwan, for help with the comet assay, and Dr. Hank Wu from Institute of Statistical Science, Academia Sinica, Taiwan, for the

statistical analysis of comet tail moment. This work was partially supported by the U.S. National Institutes of Health Research Grant AI40038 and CA 108302.

References

Bakkenist, C.J., Kastan, M.B., 2003. DNA damage activates ATM through intermolecular autophosphorylation and dimer dissociation. Nature 421 (6922), 499–506.

Barlow, C., Ribaut-Barassin, C., Zwingman, T.A., Pope, A.J., Brown, K.D., Owens, J.W., Larson, D., Harrington, E.A., Haeberle, A.M., Mariani, J., Eckhaus, M., Herrup, K., Bailly, Y., Wynshaw-Boris, A., 2000. ATM is a cytoplasmic protein in mouse brain required to prevent lysosomal accumulation. Proc. Natl. Acad. Sci. U. S. A. 97 (2), 871–876.

Barzilai, A., Rotman, G., Shiloh, Y., 2002. ATM deficiency and oxidative stress: a new dimension of defective response to DNA damage. DNA Repair (Amst) 1 (1), 3–25.

Bowman, T., Garcia, R., Turkson, J., Jove, R., 2000. STATs in oncogenesis. Oncogene 19 (21), 2474–2488.

Brown, K.D., Ziv, Y., Sadanandan, S.N., Chessa, L., Collins, F.S., Shiloh, Y., Tagle, D.A., 1997. The ataxia-telangiectasia gene product, a constitutively expressed nuclear protein that is not up-regulated following genome damage. Proc. Natl. Acad. Sci. U. S. A. 94 (5), 1840–1845.

Burma, S., Chen, B.P., Murphy, M., Kurimasa, A., Chen, D.J., 2001. ATM phosphorylates histone H2AX in response to DNA double-strand breaks. J. Biol. Chem. 276 (45), 42462–42467.

Buscemi, G., Perego, P., Carenini, N., Nakanishi, M., Chessa, L., Chen, J., Khanna, K., Delia, D., 2004. Activation of ATM and Chk2 kinases in relation to the amount of DNA strand breaks. Oncogene 23 (46), 7691–7700.

Celeste, A., Fernandez-Capetillo, O., Kruhlak, M.J., Pilch, D.R., Staudt, D.W., Lee, A., Bonner, R.F., Bonner, W.M., Nussenzweig, A., 2003. Histone H2AX phosphorylation is dispensable for the initial recognition of DNA breaks. Nat. Cell Biol. 5 (7), 675–679.

Chen, G., Lee, E., 1996. The product of the ATM gene is a 370-kDa nuclear phosphoprotein. J. Biol. Chem. 271 (52), 33693–33697.

Chowdhury, D., Keogh, M.C., Ishii, H., Peterson, C.L., Buratowski, S., Lieberman, J., 2005. gamma-H2AX dephosphorylation by protein phosphatase 2A facilitates DNA double-strand break repair. Mol. Cell 20 (5), 801–809.

Crooks, G.E., Hon, G., Chandonia, J.M., Brenner, S.E., 2004. WebLogo: a sequence logo generator. Genome Res. 14 (6), 1188–1190.

Deng, L., Nagano-Fujii, M., Tanaka, M., Nomura-Takigawa, Y., Ikeda, M., Kato, N., Sada, K., Hotta, H., 2006. NS3 protein of hepatitis C virus associates with the tumour suppressor p53 and inhibits its function in an NS3 sequence-dependent manner. J. Gen. Virol. 87 (Pt 6), 1703–1713.

Ferri, C., Caracciolo, F., Zignego, A.L., La Civita, L., Monti, M., Longombardo, G., Lombardini, F., Greco, F., Capochiani, E., Mazzoni, A., et al., 1994. Hepatitis C virus infection in patients with non-Hodgkin's lymphoma. Br. J. Haematol. 88 (2), 392–394.

Foy, E., Li, K., Sumpter Jr., R., Loo, Y.M., Johnson, C.L., Wang, C., Fish, P.M., Yoneyama, M., Fujita, T., Lemon, S.M., Gale Jr., M., 2005. Control of antiviral defenses through hepatitis C virus disruption of retinoic acid-inducible gene-I signaling. Proc. Natl. Acad. Sci. U. S. A. 102 (8), 2986–2991.

Frank, D.A., 1999. STAT signaling in the pathogenesis and treatment of cancer. Mol. Med. 5 (7), 432–456.

Gately, D.P., Hittle, J.C., Chan, G.K., Yen, T.J., 1998. Characterization of ATM expression, localization, and associated DNA-dependent protein kinase activity. Mol. Biol. Cell 9 (9), 2361–2374.

Gattiker, A., Gasteiger, E., Bairoch, A., 2002. ScanProsite: a reference implementation of a PROSITE scanning tool. Appl. Bioinformatics 1 (2), 107–108.

Goodarzi, A.A., Jonnalagadda, J.C., Douglas, P., Young, D., Ye, R., Moorhead, G.B., Lees-Miller, S.P., Khanna, K.K., 2004. Autophosphorylation of ataxia-telangiectasia mutated is regulated by protein phosphatase 2A. EMBO J. 23 (22), 4451–4461.

Guo, J.T., Bichko, V.V., Seeger, C., 2001. Effect of alpha interferon on the hepatitis C virus replicon. J. Virol. 75 (18), 8516–8523.

Higuchi, R., Krummel, B., Saiki, R.K., 1988. A general method of in vitro preparation and specific mutagenesis of DNA fragments: study of protein and DNA interactions. Nucleic Acids Res. 16 (15), 7351–7367.

Kuiken, C., Yusim, K., Boykin, L., Richardson, R., 2005. The Los Alamos hepatitis C sequence database. Bioinformatics 21 (3), 379–384.

Lee, K.J., Choi, J., Ou, J.H., Lai, M.M., 2004. The C-terminal transmembrane domain of hepatitis C virus (HCV) RNA polymerase is essential for HCV replication in vivo. J. Virol. 78 (7), 3797–3802.

Li, K., Foy, E., Ferreon, J.C., Nakamura, M., Ferreon, A.C., Ikeda, M., Ray, S.C., Gale Jr., M., Lemon, S.M., 2005a. Immune evasion by hepatitis C virus NS3/4A protease-mediated cleavage of the Toll-like receptor 3 adaptor protein TRIF. Proc. Natl. Acad. Sci. U. S. A. 102 (8), 2992–2997.

Li, X.D., Sun, L., Seth, R.B., Pineda, G., Chen, Z.J., 2005b. Hepatitis C virus protease NS3/4A cleaves mitochondrial antiviral signaling protein off the mitochondria to evade innate immunity. Proc. Natl. Acad. Sci. U. S. A. 102 (49), 17717–17722.

Lim, D.S., Kirsch, D.G., Canman, C.E., Ahn, J.H., Ziv, Y., Newman, L.S., Darnell, R.B., Shiloh, Y., Kastan, M.B., 1998. ATM binds to beta-adaptin in cytoplasmic vesicles. Proc. Natl. Acad. Sci. U. S. A. 95 (17), 10146–10151.

Machida, K., Cheng, K.T., Sung, V.M., Lee, K.J., Levine, A.M., Lai, M.M., 2004. Hepatitis C virus infection activates the immunologic (type II) isoform of nitric oxide synthase and thereby enhances DNA damage and mutations of cellular genes. J. Virol. 78 (16), 8835–8843.

Machida, K., Cheng, K.T., Lai, C.K., Jeng, K.S., Sung, V.M., Lai, M.M., 2006. Hepatitis C virus triggers mitochondrial permeability transition with production of reactive oxygen species, leading to DNA damage and STAT3 activation. J. Virol. 80 (14), 7199–7207.

Meylan, E., Curran, J., Hofmann, K., Moradpour, D., Binder, M., Bartenschlager, R., Tschopp, J., 2005. Cardif is an adaptor protein in the RIG-I antiviral pathway and is targeted by hepatitis C virus. Nature 437 (7062), 1167–1172.

Motoyama, N., Naka, K., 2004. DNA damage tumor suppressor genes and genomic instability. Curr. Opin. Genet. Dev. 14 (1), 11–16.

Muramatsu, S., Ishido, S., Fujita, T., Itoh, M., Hotta, H., 1997. Nuclear localization of the NS3 protein of hepatitis C virus and factors affecting the localization. J. Virol. 71 (7), 4954–4961.

Narayanan, A., Wu, X., Yang, Z.R., 2002. Mining viral protease data to extract cleavage knowledge. Bioinformatics 18 (Suppl 1), S5–S13.

Oka, A., Takashima, S., 1998. Expression of the ataxia-telangiectasia gene (ATM) product in human cerebellar neurons during development. Neurosci. Lett. 252 (3), 195–198.

Rogakou, E.P., Boon, C., Redon, C., Bonner, W.M., 1999. Megabase chromatin domains involved in DNA double-strand breaks in vivo. J. Cell Biol. 146 (5), 905–916.

Rothkamm, K., Lobrich, M., 2003. Evidence for a lack of DNA double-strand break repair in human cells exposed to very low x-ray doses. Proc. Natl. Acad. Sci. U. S. A. 100 (9), 5057–5062.

Saito, I., Miyamura, T., Ohbayashi, A., Harada, H., Katayama, T., Kikuchi, S., Watanabe, Y., Koi, S., Onji, M., Ohta, Y., et al., 1990. Hepatitis C virus infection is associated with the development of hepatocellular carcinoma. Proc. Natl. Acad. Sci. U. S. A. 87 (17), 6547–6549.

Shepard, C.W., Finelli, L., Alter, M.J., 2005. Global epidemiology of hepatitis C virus infection. Lancet, Infect. Dis. 5 (9), 558–567.

Shiloh, Y., 2003. ATM and related protein kinases: safeguarding genome integrity. Nat. Rev., Cancer 3 (3), 155–168.

Shiloh, Y., Kastan, M.B., 2001. ATM: genome stability, neuronal development, and cancer cross paths. Adv. Cancer Res. 83, 209–254.

Sung, V.M., Shimodaira, S., Doughty, A.L., Picchio, G.R., Can, H., Yen, T.S., Lindsay, K.L., Levine, A.M., Lai, M.M., 2003. Establishment of B-cell lymphoma cell lines persistently infected with hepatitis C virus in vivo and in vitro: the apoptotic effects of virus infection. J. Virol. 77 (3), 2134–2146.

Taneja, N., Davis, M., Choy, J.S., Beckett, M.A., Singh, R., Kron, S.J., Weichselbaum, R.R., 2004. Histone H2AX phosphorylation as a predictor of radiosensitivity and target for radiotherapy. J. Biol. Chem. 279 (3), 2273–2280.

Thompson, J.D., Higgins, D.G., Gibson, T.J., 1994. CLUSTAL W: improving the sensitivity of progressive multiple sequence alignment through sequence weighting, position-specific gap penalties and weight matrix choice. Nucleic Acids Res. 22 (22), 4673–4680.

Tu, H., Gao, L., Shi, S.T., Taylor, D.R., Yang, T., Mircheff, A.K., Wen, Y., Gorbalenya, A.E., Hwang, S.B., Lai, M.M., 1999. Hepatitis C virus RNA polymerase and NS5A complex with a SNARE-like protein. Virology 263 (1), 30–41.

Watters, D., Kedar, P., Spring, K., Bjorkman, J., Chen, P., Gatei, M., Birrell, G., Garrone, B., Srinivasa, P., Crane, D.I., Lavin, M.F., 1999. Localization of a portion of extranuclear ATM to peroxisomes. J. Biol. Chem. 274 (48), 34277–34282.

Wolk, B., Sansonno, D., Krausslich, H.G., Dammacco, F., Rice, C.M., Blum, H.E., Moradpour, D., 2000. Subcellular localization, stability, and *trans*-cleavage competence of the hepatitis C virus NS3–NS4A complex expressed in tetracycline-regulated cell lines. J. Virol. 74 (5), 2293–2304.

Young, D.B., Jonnalagadda, J., Gatei, M., Jans, D.A., Meyn, S., Khanna, K.K., 2005. Identification of domains of ataxia-telangiectasia mutated required for nuclear localization and chromatin association. J. Biol. Chem. 280 (30), 27587–27594.